Journal of Power Sources 196 (2011) 10658–10666

Contents lists available at ScienceDirect

Journal of Power Sources

journal homepage: www.elsevier.com/locate/jpowsour

Functionalized ionic liquids based on guanidinium cations with two ether groups as new electrolytes for lithium battery

Yide Jin [a], Shaohua Fang [a,*], Li Yang [a,*], Shin-ichi Hirano [b], Kazuhiro Tachibana [c]

[a] School of Chemistry and Chemical Technology, Shanghai Jiaotong University, Shanghai 200240, China
[b] Hirano Institute for Materials Innovation, Shanghai Jiaotong University, Shanghai 200240, China
[c] Department of Chemistry and Chemical Engineering, Faculty of Engineering, Yamagata University, Yamagata 992-8510, Japan

ARTICLE INFO

Article history:
Received 3 May 2011
Received in revised form 30 June 2011
Accepted 2 August 2011
Available online 9 August 2011

Keywords:
Lithium battery
Ionic liquid
Electrolyte
Functionalized cation

ABSTRACT

Two new functionalized ionic liquids (ILs) based on guanidinium cation with two ether groups and $TFSA^-$ anion are synthesized and characterized. Their physicochemical and electrochemical properties, including melting point, thermal stability, density, viscosity, conductivity, and electrochemical window are determined. Both the ILs are liquids at room temperature, and the viscosities are about 60 mPa s at 25 °C. Behavior of lithium redox, chemical stability against lithium metal and charge–discharge characteristics of lithium battery, are also examined for the two ILs as electrolyte with 0.6 mol kg^{-1} LiTFSA. Though the cathodic limiting potentials of the two ILs are higher than 0 V versus Li/Li^+, the lithium plating and stripping on Ni electrode can be observed in the two IL electrolytes, indicating their good chemical stability against lithium metal. $Li/LiFePO_4$ cells using the two IL electrolytes without any additive showed good cycle property at the current rate of 0.2 C at 25 °C and 55 °C.

1. Introduction

Ionic liquids (ILs) are molten salts with melting points at or below ambient temperature, which are consisted of various cations and anions. ILs have been attracted great interests because of their superior properties, such as non-volatility, non-flammability, good thermal stability, excellent electrochemical stability and high ionic conductivity [1–3]. ILs have showed potential as safe electrolytes for high energy density lithium metal battery, which with high theoretical capacity of 3860 mAh g^{-1} [4–7]. So far, imidazolium [8–13], quaternary ammonium [14–17], piperidinium [4,18–20], pyrrolidinium [6,21–23] and guanidinium [24,25] based ILs have been studied as new electrolytes for lithium battery.

To date, functionalized IL is a very noticeable topic in the field of IL research. By introducing different functional groups into IL cations, the physicochemical and electrochemical properties of ILs are observably changed, and providing more choices for applications as electrolytes for electrochemical devices [26,27]. Nitrile-functionalized ILs are important series of functionalized ILs, and nitrile-functionlized imidazolium, pyridinium, and quaternary ammonium ILs have been synthesized, and these ILs own good electrochemical stability [28–30]. The nitrile-functionalized imidazolium and quaternary ammonium ILs have been applied as electrolytes in lithium battery, but the battery performances are not so good due to the high viscosity [14,31]. The imidazolium, pyrrolidinium, piperidinium and morpholinium ILs with ester group also show wide electrochemical window, and have been used as additives of organic electrolyte for lithium battery [32]. Besides nitrile- and ester-functionalized ILs, ether-functionalized ILs have been investigated intensively. Compared with other functional groups, incorporating one short ether group into cations can help to reduce the viscosities and melting points, and not cause the degradation of electrochemical stability of the ILs [33–36]. One ether group has already been introduced into cations, such as imidazolium [34,37,38], quaternary ammonium [35,39–41], pyrrolidinium [36], piperidinium [36,40], morpholinium [36], oxazolidinium [36], guanidinium [25,42], sulfonium [43] and quaternary phosphonium [41]. And some of them have been researched as new electrolytes for electrochemical devices. The N,N-diethyl-N-methyl-N-(2-methoxyethyl) ammonium bis(trifluoromethanesulfonyl) imide (DEME-TFSA) and triethyl(2-methoxyethyl) phosphonium bis(trifluoromethanesulfonyl) imide (P222(2o1)-TFSA) IL electrolytes lithium battery with good cycle performances at low current rate have been reported [44–48], and polymer (PVDF-HFP) gel electrolytes containing N-methoxyethyl-N-methylpyrrolidinium bis(trifluoromethanesulfonyl)imide (PY1(2o1)-TFSA) have been described to possess good capacity and cycle property at medium C-rates [49]. The DEME-BF_4 electrolyte used for Electric double layer capacitor exhibits remarkable cycle performance even at temperature over 100 °C [50,51]. And 3-[2-(2-methoxyethoxy)ethyl]-1-methyl imidazolium

* Corresponding authors. Tel.: +86 21 54748917; fax: +86 21 54741297.
E-mail addresses: housefang@sjtu.edu.cn (S. Fang), liyangce@sjtu.edu.cn (L. Yang).

0378-7753/$ – see front matter © 2011 Published by Elsevier B.V.
doi:10.1016/j.jpowsour.2011.08.008

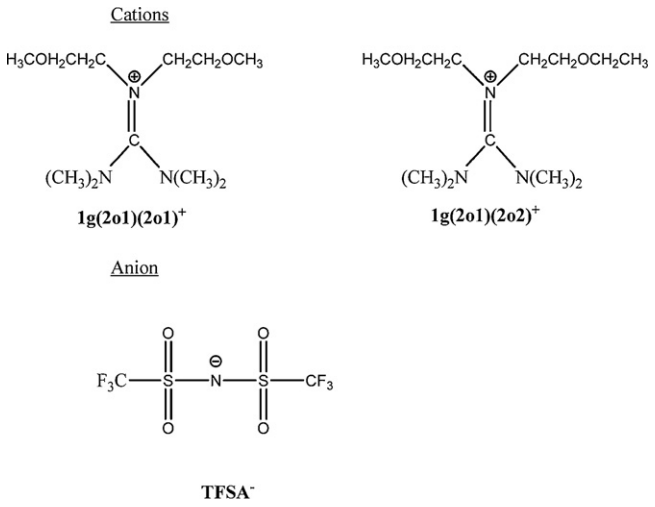

Fig. 1. Structures of cation and anion of functionalized guanidinium ILs with two ether groups used in this study.

iodide (MEOII) have been applied in dye-sensitized solar cells [52].

In contrast to the ILs with one ether group, researches involving the ILs with two or more ether groups are quite rare. A series of symmetrical dialkoxymethyl-substituted imidazolium ILs have been reported, but the viscosities of these ILs are higher than 80 mPa s at 25 °C due to long chains of ether groups [53]. Several quaternary ammonium ILs based on cations with two identical ether groups (2-ethoxyethyl or 4-methoxybenzyl group) are synthesized, and the thermal properties of these ILs have been investigated [54]. Recently, some quaternary ammonium ILs comprised of multi identical ether groups (2-methoxyethyl group) in cation are prepared, and their properties have been studied [55]. And our group also has prepared pyrrolidinium and piperidinium ILs with two ether groups and quaternary ammonium ILs with three or four different ether groups, and their possibility as electrolytes for lithium battery at low rate are also explored [56,57].

During the past two years, sixteen ILs based on small guanidinium cations without functional groups and $TFSA^-$ anion, and eight functionalized ILs based on the guanidinium cations with one ether group (2-methoxyethyl group) or ester group (methyl acetate group) and $TFSA^-$ anion have been synthesized by our group, and some of them show low viscosity and good electrochemical stability [42,58]. It has been found that two guanidinium ILs without functional groups (1g13-TFSA and 1g22-TFSA) and the gunidinium IL with one ether group (1g1(2o1)-TFSA) are able to use as electrolytes for $Li/LiCoO_2$ cells without additive [24,25]. In the present study, two new ILs based on guanidinium cations with two ether groups (2-methoxyethyl group or 2-ethoxyethyl group) and $TFSA^-$ anion had been synthesized. The structures of the ILs are shown in Fig. 1. The melting point, thermal stability, viscosity, conductivity and electrochemical properties of the ILs and IL electrolytes containing 0.6 mol kg^{-1} LiTFSA had been determined. Behavior of lithium redox on Ni electrode and chemical stability against lithium metal were also investigated for the IL electrolytes. We also examined the charge–discharge characteristics of the $Li/LiFePO_4$ cells using these IL electrolytes, and found that the cells had good cycle property at the current rate of 0.2 C at 25 °C and 55 °C.

2. Experimental

2.1. Synthesis and characterization of the ILs

Guanidines with one ether group were prepared according to the reference methods [59–62], and then the guanidines were respectively reacted with 2-methoxyethyl bromide or 2-ethoxyethyl bromide in anhydrous acetonitrile for more than 48 h at 60 °C. Functionalized guanidinium bromides with two ether groups were obtained after washing with ether. They were dissolved in ethanol, and then purified with the activated carbon. After filtration, the collected solution was evaporated under reduced pressure to remove the solvent. After drying in vacuum at 50 °C for 24 h, the produced bromides and LiTFSA (kindly provided by Mortia Chemical Industries Co., Ltd.) were dissolved in deionized water and mixed for 12 h at ambient temperature. The crude ILs were dissolved with dichloromethane, and washed with deionized water until no residual halide anions in the water used to rinse the ILs were detected with $AgNO_3$. The dichloromethane was removed by rotating evaporation. The two produced ILs were dried under high vacuum for more than 48 h at 110 °C. The water content of the dried ILs was detected by a moisture titrator (Metrohm 73KF coulometer) basing on Karl-Fischer method, and the value was bellow 50 ppm. The structures of synthesized ILs were confirmed by ^1H NMR and ^{13}CNMR (Avance III 400), and chloroform-d for all ILs. The characterization data are as follows:

1g(2o1)(2o1)-TFSA: ^1H NMR: δ (ppm) 3.61-3.30 (m,14H), 2.98-2.93 (d,12H); ^{13}C NMR: δ (ppm) 164.51, 124.88-115.21, 68.68, 58.82, 49.35, 40.28, 39.88; *1g(2o1)(2o2)-TFSA*: ^1H NMR: δ (ppm) 3.66-3.31 (m,13H), 3.01-2.94 (d,12H), 1.15-1.11 (t,3H); ^{13}C NMR: δ (ppm) 164.62, 124.94-115.34, 68.74, 66.70, 58.82, 49.54, 40.11, 15.06.

2.2. Measurements

The density was affirmed by measuring the weight of prepared IL (1.0 ml) at 25 °C. The melting point of each IL was analyzed by using a differential scanning calorimeter (DSC, Perkin Elmer Pyris 1) in the temperature range of −60 °C to a predetermined temperature. The sample was sealed in aluminum pan, after that then heated and cooled at a scan fate of 10 °C min^{-1} under a flow of nitrogen. The thermal stabilities were measured with thermal gravimetric analysis (Perkin Elmer, 7 series thermal analysis system). The sample was placed in the aluminum pan and heated at 10 °C min^{-1} from ambient temperature to 600 °C under nitrogen. The viscosities of the ILs and IL electrolytes were tested with viscometer (DV-III ULTRA, Brookfield Engineering Laboratories, Inc.), and the conductivities were got from DDS-11A conductivity meter.

Electrochemical windows of the ILs were tested by linear sweep voltammogramms (LSV, scan rate 10 mV s^{-1}) in an argon-filled UNILAB glove box ($[O_2] < 1$ ppm, $[H_2O] < 1$ ppm). The working electrode was glassy carbon disk (3 mm diameter), and lithium metal was used as both counter and reference electrodes. The plating and stripping behaviors of lithium in the IL electrolytes was determined by using cyclic voltammogramms (CV, scan rate 10 mV s^{-1}) method in the glove box. The nickel disk (2 mm diameter) was used as the working electrode and lithium metal was used as both counter and reference electrodes. The nickel electrode was polished in the usage of alumina paste ($d = 0.1$ μm). And the Ni electrode was washed by deionized water then dried under vacuum. The LSV and CV tests were performed by CHI660D electrochemistry workstation at room temperature (25 °C).

The stability of the IL electrolytes against lithium metal at room temperature was investigated by monitoring the time evolution of the impedance response for a symmetric Li/IL electrolyte/Li coin cell with the borosilicate glass separator (GF/A, Whatman), and the impedance responses were measured by using CHI660D electrochemistry workstation (100 KHz–100 mHz; applied voltage 5 mV).

$Li/LiFePO_4$ coin cell was used to evaluate the performances of the IL electrolytes in lithium battery applications. Lithium foil (battery grade) was used as a negative electrode and the positive electrode was fabricated by spreading the mixture of $LiFePO_4$, acetylene black

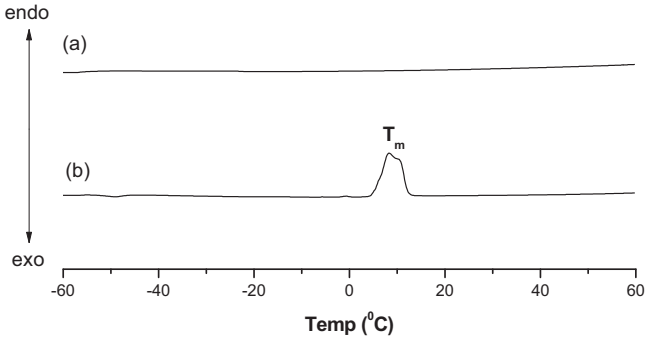

Fig. 2. DSC curves of (a) 1g(2o1)(2o1)-TFSA and (b) 1g(2o1)(2o2)-TFSA.

and PVDF (firstly dissolved in N-methyl-N-2-pyrrolidone) with a weight ratio of 8:1:1 on aluminum current collector (battery use). Loading of active materials was about ca. 1.5–2.0 mg cm^{-2} and this thinnish electrode was used without pressing. The separator was glass filter made of borosilicate glass (GF/A, Whatman). Cell was assembled in the glove box, and all the components of cell were dried under vacuum before using. Cell performances were examined by the charge–discharge (C–D) cycling tests using a CT2001A cell test instrument (LAND Electronic Co., Ltd.) at 25 °C or 55 °C and at different current rates (0.2 C–2.0 C), current rate was determined by using the nominal capacity of 150 mA h g^{-1} for Li/LiFePO$_4$ cell. The cells were sealed and then stayed at room temperature for 4 h before the performance tests. Constant current charge–discharge cycles were conducted between 2.5 and 4.0 V (versus Li/Li$^+$). Charging included two processes: (1) constant current at a rate, cut-off voltage of 4.0 V; (2) constant voltage at 4.0 V, held for 0.5 h. And discharging had one process: constant current at the same rate, cut-off voltage of 2.5 V.

3. Results and discussion

3.1. Physicochemical and electrochemical properties of the ILs and IL electrolytes

3.1.1. Thermal properties

The physical and thermal properties of the functionalized guanidinium ILs with two ether groups, including melting point (T_m), thermal decomposition temperature (T_d), density, viscosity and conductivity are listed in Table 1.

The phase transitions of the two ILs and their IL electrolytes with 0.6 mol kg^{-1} LiTFSA were measured by differential scanning calorimetry (DSC), and the DSC curves of them are illustrated in Fig. 2 as examples. The 1g(2o1)(2o2)-TFSA owned the melting point of 8.4 °C, 1g(2o1)(2o1)-TFSA and the two IL electrolytes did not show any phase transition behaviors until −60 °C, which was the interior temperature limit of our DSC measurement.

Incorporating one short ether group, such as methoxymethyl (–CH_2OCH_3) or 2-methoxyethyl (–$CH_2CH_2OCH_3$) into imidazolium [34,37,38], quaternary ammonium and phosphonium [35,40,41], pyrrolidinium [36], piperidinium [35,36], and guanidinium [25,42] cations, has been proved to be beneficial for lowing the melting points of these ILs. When two or more ether groups were introduced to imidazolium [53], quaternary ammonium [55,56], pyrrolidinium and piperidinium [57], these ILs also owned low melting points. The utilization of flexible ether groups could reduce ion symmetry, increase the ions conformational degrees of freedom, and weaken electrostatic interaction between the cation and anion, which resulted from the electron-donating action of ether group. So it was effective approach to reduce the lattice energy of the ILs, and led to low melting point ILs [63–65]. The two guanidinium ILs with two ether groups also had low melting points. Though the 1g(2o1)(2o2)-TFSA IL had lower molecular symmetry than 1g(2o1)(2o1)-TFSA, the former had higher melting point because of it had the larger molecular size, which resulted in stronger Van der Waals interaction forces that could induce the higher melting point.

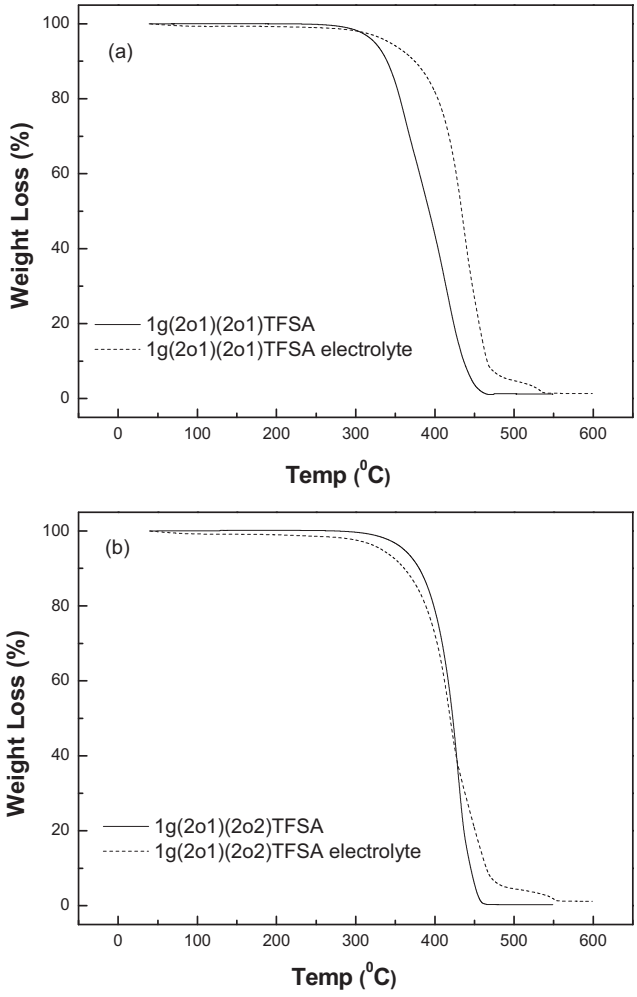

Fig. 3. TGA traces of (a) 1g(2o1)(2o1)-TFSA, 1g(2o1)(2o1)-TFSA electrolyte with 0.6 mol kg^{-1} LiTFSA, (b)1g(2o1)(2o2)-TFSA, 1g(2o1)(2o2)-TFSA electrolyte with 0.6 mol kg^{-1} LiTFSA.

Usually when the lithium salt added into the ILs to form IL electrolytes, the melting points of the IL electrolytes were lower than the ILs, such as P13-TFSA (N-propyl-N-methylpyrrolidinium TFSA) electrolyte and P14-FSA (N-butyl-N-methylpyrrolidinium FSA) electrolyte [66,67]. Likewise, the 1g(2o1)(2o2)-TFSA electrolyte showed the melting point less than −60 °C, while the T_m of 1g(2o1)(2o2)-TFSA was 8.4 °C.

The thermal stability of the ILs and IL electrolytes was measured by thermogravimetry (TG). As shown in Fig. 3, all of them had one-stage decomposition behavior. Generally the thermal decomposition temperature (T_d) of ILs with TFSA$^-$ anion decreased after introducing ether groups into IL cations [42,55–57]. When two ether groups were introduced into guanidinium cations, the T_d of ILs decreased with the increasing number of ether groups compared to the guanidinium ILs with or without one ether group. And the thermal stability of the IL with one 2-methoxyethyl and one 2-ethoxyethyl group was better than the IL with two 2-methoxyethyl groups. For example, the thermal decomposition temperature decreased in the following order: 1g1(2o1)-TFSA

Table 1
Physical and thermal properties of the ILs.

ILs	Mw[a] (g mol^{-1})	T_m[b] (°C)	d[c] (g cm^{-3})	C[d] (mol dm^{-3})	η[e] (mPa s)	σ[f] (mS cm^{-1})	Λ[g] (S cm^2 mol^{-1})	T_d[h] (°C)
1g2o1-2o1TFSA	512.49	<−60	1.22	2.38	60.2	1.66	0.70	340.1
1g2o1-2o2TFSA	526.52	8.4	1.28	2.43	58.8	1.64	0.67	380.0

[a] Molecular weight.
[b] Melting point.
[c] Density at 25 °C.
[d] Concentration at 25 °C.
[e] Viscosity at 25 °C.
[f] Conductivity at 25 °C.
[g] Molar conductivity at 25 °C.
[h] Decomposition temperature of 10% weight loss.

(425.4 °C [42] > 1g(2o1)(2o2)-TFSA (380.1 °C) > 1g(2o1)(2o1)-TFSA (340.0 °C). And the thermal decomposition temperatures of the guanidinium ILs with two ether groups was close to the quaternary ammonium [55], pyrrolidinium and piperidinium [57] ILs with two ether groups. Although the introduction of ether groups into cation structure caused adverse effect to the thermal stability of ILs, the T_d of these two guanidinium ILs with two ether groups were still higher than 300 °C.

The thermal decomposition temperatures of the two IL electrolytes also changed with the addition of lithium salt. The 1g(2o1)(2o1)-TFSA electrolyte showed a higher thermal decomposition temperature (374.2 °C) than 1g(2o1)(2o1)-TFSA, and the 1g(2o1)(2o2)-TFSA electrolyte showed a lower thermal decomposition temperature (361.2 °C) than 1g(2o1)(2o2)-TFSA.

3.1.2. Viscosity

The viscosity of IL is an important feature in the application of IL electrolyte for lithium battery. Replacing one alkyl group in the IL cations by one flexible ether group with the similar size and formula weight, could reduce the viscosity of ILs, owing to weakening the electrostatic interaction between cation and anion which resulted from the electron donation action of ether group [35,36,40–42]. And when two ether groups were introduced into guanidinium cations, the viscosities of 1g(2o1)(2o1)-TFSA and 1g(2o1)(2o2)-TFSA (60.2 mPa s and 58.8 mPa s at 25 °C) were close to the guanidinium ILs with one ether group (1g1(2o1)-TFSA, 58 mPa s at 25 °C [42]). Though the cation sizes and formula weights increased with the more ether groups, which could result in the stronger Van der Waals interactions between cations and anions, the electron donation action of the two ether groups might counteract of it. By contrast with imidazolium ILs with two identical ether groups [53], 1g(2o1)(2o1)-TFSA and 1g(2o1)(2o2)-TFSA owned lower viscosities because of choosing the shorter ether groups. And the viscosities of these two ILs were close to the pyrrolidinium ILs with two ether groups [57], lower than the piperidinium ILs with two ether groups [57] and the quaternary ammonium ILs with two or more ether groups [55].

The addition of lithium salt LiTFSA increased the viscosities of the two ILs electrolytes. The viscosity of 1g(2o1)(2o1)-TFSA electrolyte was 192.1 mPa s at 25 °C and the viscosity of 1g(2o1)(2o2)-TFSA electrolyte was 182.2 mPa s at 25 °C. Similar phenomenon existed in BMMI-TFSA (1-butyl-2,3-dimethylimidazolium TFSA) electrolyte, EtO(CH_2)$_2$MMI-TFSA (1-ethoxyethyl-2,3-dimethylimidazolium TFSA), EtO(CH_2)$_2$MMor-TFSA (N-ethoxyethyl-Nmethylmorpholinium TFSA) electrolytes [68,69].

Fig. 4a shows the temperature dependence of viscosity (η) for these two ILs and IL electrolytes over the temperature range of 25–80 °C, and the η (T) behavior was fitted by a Vogel-Tammann-Fulcher (VTF) equation (1):

$$\eta = \eta_0 \exp\left(\frac{B}{T - T_0}\right) \quad (1)$$

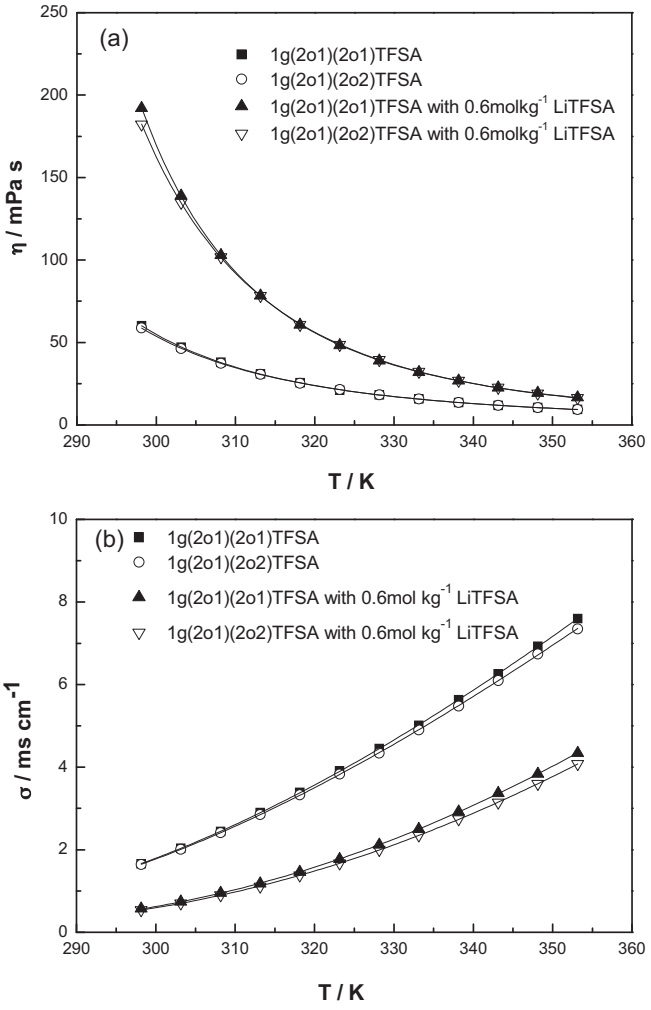

Fig. 4. Change of (a) viscosity and (b) conductivity with temperature for 1g(2o1)(2o1)-TFSA, 1g(2o1)(2o2)-TFSA and their electrolytes.

where η_o (mPa s), B (K) and T_0 (K) are adjustable parameters, these three values and the VTF fitting parameter (R^2) for the ILs and IL electrolytes were calculated and listed in Table 2. According to Fig. 4(a) and the values of R^2 in Table 2, the ILs and IL electrolytes were well fitted by the VTF model over the temperature range studied.

3.1.3. Conductivity

Conductivity measurements could be mainly influenced by the viscosity, formula weight and density of ILs [35,36,63]. Usually the ILs with low viscosity possessed high conductivity, substituting one alkyl group in the cation structure by one flexible ether group with

Table 2
VTF equation parameters of viscosity for the ILs and IL electrolytes.

ILs and IL electrolytes	η_0 (mPa s)	B (K)	T_0 (K)	R^2
1g(2o1)(2o1)TFSA	0.20 (±2%)	640.0 (±7%)	169.3 (±2%)	0.9999
1g(2o1)(2o2)TFSA	0.18 (±9%)	677.4 (±3%)	180.6 (±1%)	0.9999
1g(2o1)(2o1)TFSA electrolyte	0.17 (±8%)	716.1 (±3%)	196.0 (±1%)	0.9999
1g(2o1)(2o2)TFSA electrolyte	0.07 (±12%)	987.6 (±3%)	173.2 (±1%)	0.9999

The percentage standard errors for η_0, B and T_0 have been included, and R^2 is the VTF fitting parameter.

similar size and formula weight, could increase the conductivity of IL [34–36,41,42,63]. The conductivity of 1g(2o1)(2o1)-TFSA was 1.66 mS cm^{-1} at 25 °C and 1g(2o1)(2o2)-TFSA was 1.64 mS cm^{-1} at 25 °C. Comparing with the conductivity of guanidinium ILs with or without one short ether group (1g1(2o1)-TFSA, 2.15 mS cm^{-1} at 25 °C [42]; 1g14-TFSA, 1.91 mS cm^{-1} at 25 °C [24]), the two ILs with two ether groups had lower conductivities, due to the bigger cation sizes and formula weights which counteracted the electron donation action of more ether groups. In contrast to the piperidinium ILs with two ether groups [57] and the quaternary ammonium ILs with two or more ether groups [55], the conductivities of these two ILs were higher and might be due to the lower viscosities discussed in previous section. And the conductivities of them were lower than the pyrrolidinium ILs with two ether groups [57] despite of the viscosities of these two categories were very close.

The conductivities decreased obviously with the addition of lithium salt for the two ILs electrolytes. The conductivity of 1g(2o1)(2o1)-TFSA electrolyte was 0.57 mS cm^{-1} at 25 °C and the conductivity of 1g(2o1)(2o2)-TFSA electrolyte was 0.54 mS cm^{-1} at 25 °C.

The temperature dependence of conductivity was investigated for both ILs and IL electrolytes in the temperature range of 25–80 °C, and the VTF plots of conductivity for them according to Eq. (2) were shown in Fig. 4(b):

$$\sigma = \sigma_0 \exp\left(\frac{-B}{T - T_0}\right) \quad (2)$$

where σ_0 (mS cm^{-1}), B (K) and T_o (K) are constants of Eq. (2), and these three values and the VTF fitting parameter (R^2) for them were calculated and listed in Table 3. The temperature dependence of conductivity was also very well fitted by the VTF model over the temperature range studied.

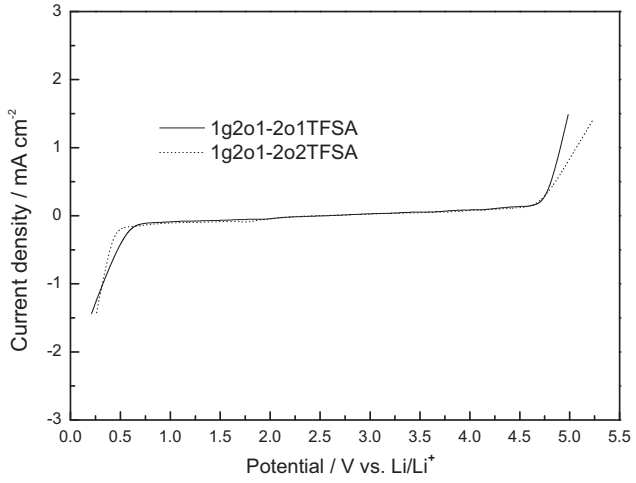

Fig. 5. Linear sweep voltammograms of 1g(2o1)(2o1)-TFSA and 1g(2o1)(2o2)-TFSA at 25 °C. Working electrode, glassy carbon; (diameter = 3 mm); counter electrode, Li; reference electrode, Li; scan rate, 10 mV s^{-1}.

3.1.4. Electrochemical window

The Linear sweep voltammogramms (LSV) using lithium metal as reference electrode for the electrochemical window measurement of the two ILs was shown in Fig. 5. The cathodic limiting potentials of 1g(2o1)(2o1)-TFSA and 1g(2o1)(2o2)-TFSA were about 0.6 V and 0.4 V versus Li/Li$^+$, and their anodic limiting potentials were about 4.7 V versus Li/Li$^+$, so the electrochemical window were 4.1 V and 4.3 V, respectively. As already reported, introducing one ether group into the cations of quaternary ammonium, pyrrolidinium and piperidinium ILs would reduce the electrochemical stability [35,36,40]. And the electrochemical stabilities of the quaternary ammonium ILs [55], pyrrolidinium ILs and piperidinium ILs [57] with two ether groups also decreased comparing with the homologous ILs without ether groups. For guanidinium ILs, it could be found that the electrochemical windows of these ILs with two ether groups were close to the guanidinium ILs with or without one

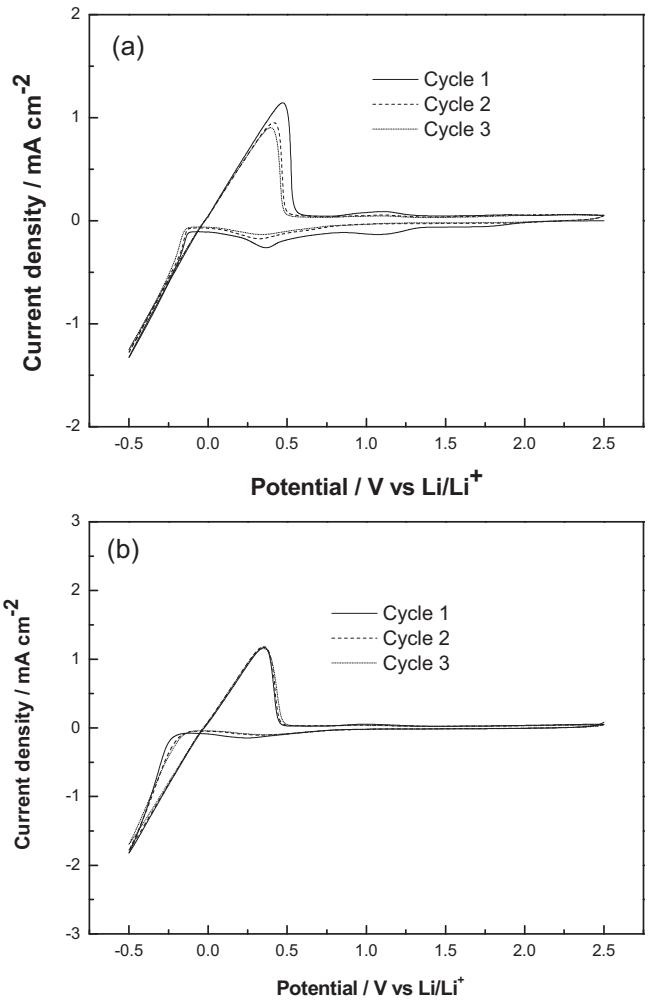

Fig. 6. Cyclic voltammograms of these IL electrolytes at 25 °C (−0.5 V to 2.5 V versus Li/Li$^+$) (a) 1g(2o1)(2o1)-TFSA electrolyte, (b) 1g(2o1)(2o2)-TFSA electrolyte. Working electrode, Ni; counter electrode, Li; reference electrode, Li; scan rate, 10 mV s^{-1}.

Table 3
VTF equation parameters of conductivity for the ILs and IL electrolytes.

ILs and IL electrolytes	σ_0 (mS cm^{-1})	B (K)	T_0 (K)	R^2
1g(2o1)(2o1)TFSA	132.5 (±2%)	453.1 (±3%)	194.6 (±1%)	0.999
1g(2o1)(2o2)TFSA	116.6 (±5%)	432.0 (±3%)	196.8 (±1%)	0.999
1g(2o1)(2o1)TFSA electrolyte	188.8 (±7%)	589.4 (±3%)	196.2 (±1%)	0.999
1g(2o1)(2o2)TFSA electrolyte	188.7 (±6%)	609.4 (±3%)	194.2 (±1%)	0.999

The percentage standard errors for σ_0, B and T_0 have been included, and R^2 is the VTF fitting parameter.

ether group [24,42]. The electrochemical windows did not change much after the ether group were introduced into the guanidinium ILs cation, which might indicate that the electrochemical stabilities of guanidinium ILs were influenced by the main structure of cation. Moreover, the electrochemical stabilities of these two ILs were close to the imidazolium and sulfonium ILs [40,70].

3.2. Lithium redox in the IL electrolytes

According to the cathodic limiting potentials of the two guanidinium ILs with two ether groups, it was very possible that their IL electrolytes could not allow the deposition of lithium without any additive like the EMI-TFSA electrolyte [40]. But the cyclic voltammogramms (CV) test obviously gave the opposite result. The CVs of the two IL electrolytes at 25 °C were shown in Fig. 6(a) and (b). The deposition and dissolution of Li on and from the Ni electrode could be clearly found in both IL electrolytes [25]. In the first cycle for the 1g(2o1)(2o1)-TFSA electrolyte, the deposition of lithium was at about −0.11 V versus Li/Li$^+$, and the anodic peak at about 0.47 V in the returning scan related to the dissolution of lithium. The lithium redox in this electrolyte might be caused by the formation of the solid electrolyte interface (SEI) on the Ni electrode surface. The peak currents of the lithium redox decreased gradually with the increasing cycle number, and it demonstrated that the SEI film changed so that the lithium redox was restrained. And the cathodic peak at about 0.36 V existed in the first cycle, it might be assigned to the electrochemical reduction of the IL electrolyte. The electrochemical reduction products could be assumed to be the generation of the SEI film on the Ni electrode. In addition, the cathodic peak value decreased in the remaining two cycles, so it could be understood that the SEI film generating in the first cycle also restrained the reduction of the electrolyte. The lithium plating and stripping behaviors on Ni electrode of the 1g(2o1)(2o2)-TFSA electrolyte were similar to the 1g(2o1)(2o1)-TFSA electrolyte.

One cathodic peak in the range from 0.8 V to 1.3 V versus Li/Li$^+$ was found in the first cycle for the 1g(2o1)(2o1)-TFSA electrolyte, which might be caused by the reactions of the trace water or oxygen in IL electrolyte on Ni electrode, and this peak disappeared in the second and third cycles because of the SEI film forming in the first cycle. This kind of cathodic peak provoked by the trace impurities, could also be found in some other IL electrolytes CV experimental results [31,71].

3.3. Chemical stabilities of the IL electrolytes against lithium metal

The Li/IL electrolyte/Li symmetric cells were used to investigate the chemical stabilities of the IL electrolyte against the lithium metal and the interfacial characteristics between the Li metal electrode and IL electrolyte by the electrochemical impedance spectra (EIS). Fig. 7(a)–(d) illustrated the time dependence of impedance spectra for Li/IL electrolyte/Li symmetric cells under the open circuit conditions. The intercept with the real axis of the response at

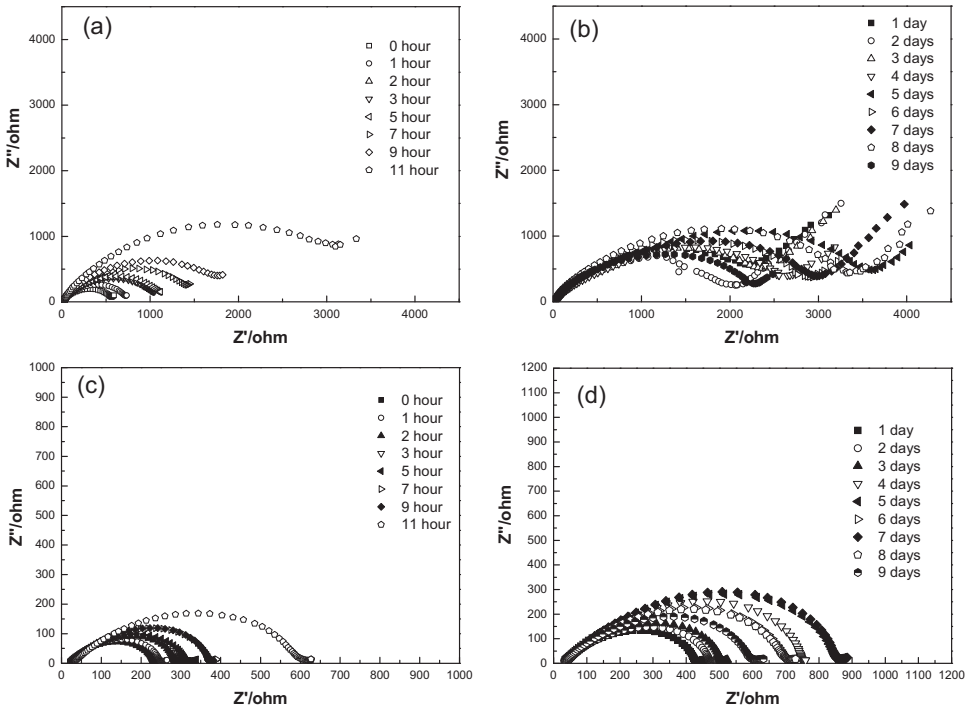

Fig. 7. Time evolution of the impedance spectra of a symmetrical Li/1g(2o1)(2o1)-TFSA electrolyte/Li cell: (a) from 0 h to 11 h, (b) from 1 day to 9 days; a symmetrical Li/1g(2o1)(2o2)-TFSA electrolyte/Li cell: (c) from 0 h to 11 h, (d) from 1 day to 9 days.

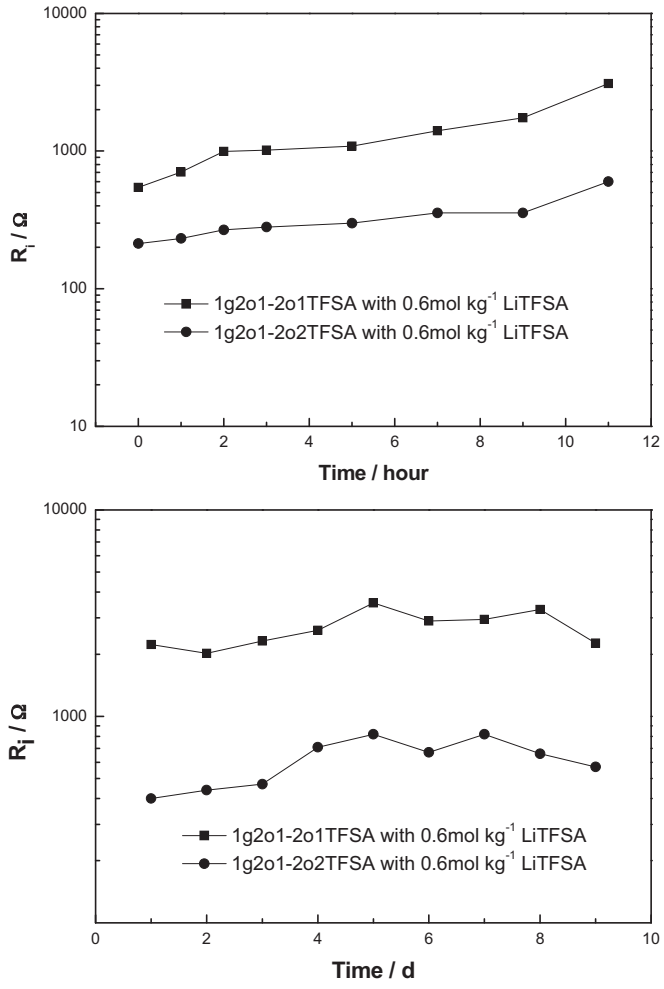

Fig. 8. Time dependence of interfacial resistance of the Li/1g(2o1)(2o1)-TFSA electrolyte/Li, Li/1g(2o1)(2o2)-TFSA electrolyte/Li cells: (a) from 0 h to 11 h; (b) from 1 day to 9 days.

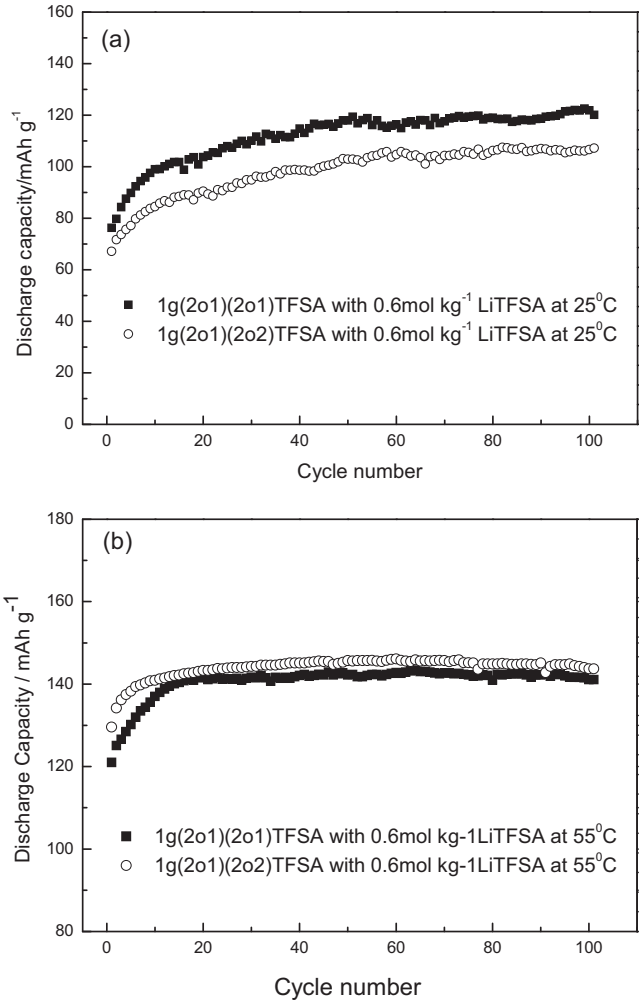

Fig. 9. Cycling performances of Li/LiFePO4 cells using the two IL electrolytes (a) at 25 °C, and (b) at 55 °C. Charge–discharge current rate is 0.2 C.

high frequency was assigned to electrolyte bulk resistance (R_{bulk}), and the diameter of the semicircle was related to the interfacial resistance (R_i) of the IL electrolyte/lithium metal, as explained in the literature [10,46,72]. For the 1g(2o1)(2o1)-TFSA electrolyte, its bulk resistance was almost unchanged during the testing period of 9 days. At first, the R_i increased gradually from 0 h to 11 h, and the R_i retained about 2200 Ω after one day. The cathodic limiting potential of 1g(2o1)(2o1)-TFSA was about 0.6 V versus Li/Li$^+$, so it was highly possible that this IL electrolyte would continuously react with lithium metal. Fortunately, the R_i only fluctuated a little from 1 day to 9 days and was stable at the level of 2300 Ω at last, which could be seen in Fig. 8a. This phenomenon might indicate that when the IL electrolyte reacted with lithium metal, a passivation film could be produced in the meantime. And the passivation film somehow restrained the reaction between the IL electrolyte and lithium metal, which leads to a dynamic equilibrium state after a period of time at last. For the 1g(2o1)(2o2)-TFSA electrolyte, a similar phenomenon of R_i variation was also illustrated in Fig. 8b, and the R_i value was stable at the level of 550 Ω at last.

3.4. Charge–discharge performances of Li/LiFePO$_4$ cells

The charge–discharge performances of Li/LiFePO$_4$ cells using the two IL electrolytes without additive were examined. Fig. 9(a) shows the discharge capacity of the two IL electrolytes containing cells cycling at 0.2 C and at 25 °C. The initial discharge capacity of the 1g(2o1)(2o1)-TFSA electrolyte was 76 mA h g^{-1} then increased gradually during the next 50 cycles and stabilized at the level of 120 mA h g^{-1} for the rest 50 cycles. The 1g(2o1)(2o2)-TFSA electrolyte delivered a smaller initial discharge capacity of 67 mA h g^{-1} and the discharge capacity increased as the former IL electrolyte, and the value retained about 107 mA h g^{-1} until the 100th cycle. The low initial discharge capacity might be influenced by the IL electrolytes poor wettability towards LiFePO$_4$ cathode material as a result of the high viscosity of them. The discharge capacity improved with the increasing cycle numbers for both the IL electrolytes, it might be due to the optimization of the electric contact between the cathode and electrolyte, the IL electrolytes penetrated the cathode pore structure gradually and finally wetted the electrode completely.

As shown in Table 4, the viscosity and conductivity of the two IL electrolytes improved obviously at 55 °C. The Li/LiFePO$_4$ cells using the two IL electrolytes cycling at 0.2 C at 55 °C delivered better discharge capacity than 25 °C, seen in Fig. 9(b). The initial discharge capacity of the 1g(2o1)(2o2)-TFSA electrolyte was 130 mA h g^{-1} then increased gradually during the next 20 cycles and stabilized at the level of 145 mA h g^{-1} for the rest 80 cycles. And the 1g(2o1)(2o1)-TFSA electrolyte delivered a smaller initial discharge capacity of 120 mA h g^{-1} then the discharge capacity also was stable after 20 cycles, and the value retained about 142 mA h g^{-1} until the

Table 4
Viscosity and conductivity of the two IL electrolytes with 0.6 mol kg^{-1} LiTFSA at 25 °C and 55 °C.

IL electrolytes	Viscosity (mPa s)		Conductivity (mS cm^{-1})	
	25 °C	55 °C	25 °C	55 °C
1g(2o1)(2o1)TFSA electrolyte	192.1	39	0.57	2.12
1g(2o1)(2o2)TFSA electrolyte	182.2	39.4	0.54	2.00

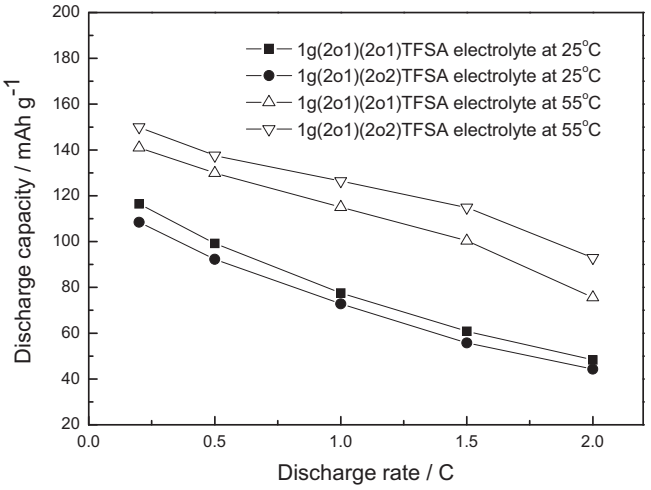

Fig. 10. Discharge capacities of Li/LiFePO$_4$ cells using the IL electrolytes at different rates at 25 °C and 55 °C. Charge and discharge current rates are 0.2, 0.5, 1.0, 1.5, 2.0 C.

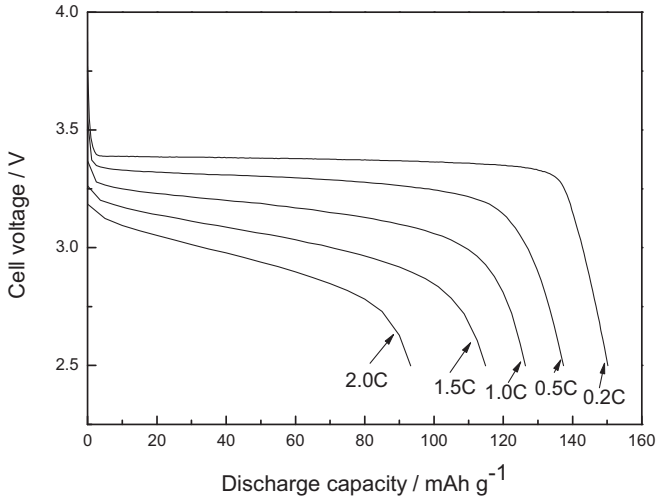

Fig. 11. Discharge capacities of Li/LiFePO$_4$ cells using 1g(2o1)(2o2)-TFSA IL electrolytes at different rates at 55 °C. Charge and discharge current rates are 0.2, 0.5, 1.0, 1.5, 2.0 C.

100th cycle. And it could be easily found that the discharge capacities of the two IL electrolytes at 55 °C went stable quicker than at 25 °C, mainly due to the improvement for viscosity and conductivity of the IL electrolytes. Furthermore, the discharge capacity of 1g(2o1)(2o1)-TFSA electrolyte was higher than 1g(2o1)(2o2)-TFSA electrolyte at 25 °C though the viscosity of the former electrolyte was higher than the latter. But the 1g(2o1)(2o2)-TFSA electrolyte delivered better discharge capacity than 1g(2o1)(2o1)-TFSA electrolyte at 55 °C despite the viscosities of the two IL electrolytes were very close. The differences for the discharge capacities of the IL electrolytes at 25 °C and 55 °C, could not only affect by the viscosities of the IL electrolytes, but also some other factors such as the interfacial characteristics at both the LiFePO$_4$ cathode/electrolyte and lithium anode/electrolyte interfaces.

The rate properties of Li/LiFePO$_4$ cells are shown in Fig. 10, and the discharge capacities at different rates are the values after the cycle performances of cells reach stability. It could be found that the discharge capacity decreased with the increasing discharge rate for these IL electrolytes, and the IL electrolytes possessed better rate properties at 55 °C. The rate property of 1g(2o1)(2o1)-TFSA electrolyte was better than 1g(2o1)(2o2)-TFSA electrolyte at 25 °C. The discharge capacity of 1g(2o1)(2o1)-TFSA electrolyte at the current rate of 1.0 C was about 78 mA h g^{-1}, which retained 67% of the capacity at the rate of 0.2 C. The 1g(2o1)(2o2)-TFSA electrolyte showed better rate property than 1g(2o1)(2o1)-TFSA electrolyte at 55 °C. As shown in Fig. 11, the discharge capacity of the 1g(2o1)(2o2)-TFSA electrolyte at the discharge rate of 1.0 C was about 125 mA h g^{-1}, which retained 87% of the discharge capacity at 0.2 C, and the discharge capacity at 2 C was about 93 mA h g^{-1}, which retained 65% of the discharge capacity at 0.2 C. The obvious difference of rate properties of the two IL electrolytes at 25 °C and 55 °C might caused by the viscosities and conductivities of them at each testing temperature, the lower viscosities and higher conductivities of the two IL electrolytes at 55 °C could be helpful to the rate property of cells, due to better transport capability of lithium ion in IL electrolyte.

4. Conclusions

Two new functionalized ILs based on guanidinium cation with two ether groups and TFSA$^-$ anion were synthesized. Both the ILs were liquids at room temperature, and the viscosities of 1g(2o1)(2o1)-TFSA and 1g(2o1)(2o2)-TFSA were 60.2 and 58.8 mPa s at 25 °C, respectively. Good electrochemical stabilities of these guanidinium ILs with two ether groups permitted them to become potential electrolytes for electrochemical devices. Though the cathodic limiting potentials of the ILs were higher than 0 V versus Li/Li$^+$, the lithium plating and stripping on Ni electrode could be found in the two IL electrolytes without additive because of the formation of SEI film. And the IL electrolytes showed good chemical stability against lithium metal owing to the formation of passivation layer. Li/LiFePO4 cells using the two IL electrolytes without additive showed good cycle property at the current rate of 0.2 C at 25 °C and 55 °C.

Acknowledgements

The authors thank the Research Center of Analysis and Measurement of Shanghai JiaoTong University for the help in NMR characterization. This work was financially supports by the National Natural Science Foundation of China (Grants No. 21103108 and 21173148).

References

[1] J. Dupont, R.F. de Souza, P.A.Z. Suarez, Chem. Rev. 102 (2002) 3667–3692.
[2] R.D. Rogers, K.R. Seddon, Science 302 (2003) 792–793.
[3] S.A. Forsyth, J.M. Pringle, D.R. MacFarlane, Aus. J. Chem. 57 (2004) 113–119.
[4] H. Sakaebe, H. Matsumoto, Electrochem. Commun. 5 (2003) 594–598.
[5] M. Egashira, M. Tanaka-Nakagawa, I. Watanabe, S. Okada, J.-i. Yamaki, J. Power Sources 160 (2006) 1387–1390.
[6] H. Matsumoto, H. Sakaebe, K. Tatsumi, M. Kikuta, E. Ishiko, M. Kono, J. Power Sources 160 (2006) 1308–1313.

[7] A. Lewandowski, I. Acznik, A. Swiderska-Mocek, J. Appl. Electrochem. 40 (2010) 1619–1624.
[8] B. Garcia, S. Lavallée, G. Perron, C. Michot, M. Armand, Electrochim. Acta 49 (2004) 4583–4588.
[9] S. Seki, Y. Kobayashi, H. Miyashiro, Y. Ohno, A. Usami, Y. Mita, N. Kihira, M. Watanabe, N. Terada, J. Phys. Chem. B 110 (2006) 10228–10230.
[10] S. Seki, Y. Ohno, Y. Kobayashi, H. Miyashiro, A. Usami, Y. Mita, H. Tokuda, M. Watanabe, K. Hayamizu, S. Tsuzuki, M. Hattori, N. Terada, J. Electrochem. Soc. 154 (2007) A173–A177.
[11] L. Zhao, J.-i. Yamaki, M. Egashira, J. Power Sources 174 (2007) 352–358.
[12] J.-K. Kim, A. Matic, J.-H. Ahn, P. Jacobsson, J. Power Sources 195 (2010) 7639–7643.
[13] H. Saruwatari, T. Kuboki, T. Kishi, S. Mikoshiba, N. Takami, J. Power Sources 195 (2010) 1495–1499.
[14] M. Egashira, S. Okada, J.-i. Yamaki, D.A. Dri, F. Bonadies, B. Scrosati, J. Power Sources 138 (2004) 240–244.
[15] M. Egashira, M. Nakagawa, I. Watanabe, S. Okada, J.-i. Yamaki, J. Power Sources 146 (2005) 685–688.
[16] H. Sakaebe, H. Matsumoto, K. Tatsumi, J. Power Sources 146 (2005) 693–697.
[17] Y. Kobayashi, Y. Mita, S. Seki, Y. Ohno, H. Miyashiro, N. Terada, J. Electrochem. Soc. 154 (2007) A677–A681.
[18] H. Sakaebe, H. Matsumoto, K. Tatsumi, Electrochim. Acta 53 (2007) 1048–1054.
[19] V. Borgel, E. Markevich, D. Aurbach, G. Semrau, M. Schmidt, J. Power Sources 189 (2009) 331–336.
[20] J. Jin, H.H. Li, J.P. Wei, X.K. Bian, Z. Zhou, J. Yan, Electrochem. Commun. 11 (2009) 1500–1503.
[21] Y. Wang, K. Zaghib, A. Guerfi, F.F.C. Bazito, R.M. Torresi, J.R. Dahn, Electrochim. Acta 52 (2007) 6346–6352.
[22] H. Ye, J. Huang, J.J. Xu, A. Khalfan, S.G. Greenbaum, J. Electrochem. Soc. 154 (2007) A1048–A1057.
[23] J.H. Shin, P. Basak, J.B. Kerr, E.J. Cairns, Electrochim. Acta 54 (2008) 410–414.
[24] S. Fang, L. Yang, J. Wang, H. Zhang, K. Tachibana, K. Kamijima, J. Power Sources 191 (2009) 619–622.
[25] S. Fang, Y. Tang, X. Tai, L. Yang, K. Tachibana, K. Kamijima, J. Power Sources 196 (2011) 1433–1441.
[26] J.H. Davis Jr., Chem. Lett. 33 (2004) 1072–1077.
[27] Z. Fei, T.J. Geldbach, D. Zhao, P.J. Dyson, Chem. - Eur. J. 12 (2006) 2122–2130.
[28] D. Zhao, Z. Fei, T.J. Geldbach, R. Scopelliti, P.J. Dyson, J. Am. Chem. Soc. 126 (2004) 15876–15882.
[29] D. Zhao, Z. Fei, R. Scopelliti, P.J. Dyson, Inorg. Chem. 43 (2004) 2197–2205.
[30] Q. Zhang, Z. Li, J. Zhang, S. Zhang, L. Zhu, J. Yang, X. Zhang, Y. Deng, J. Phys. Chem. B 111 (2007) 2864–2872.
[31] M. Egashira, H. Todo, N. Yoshimoto, M. Morita, J.-I. Yamaki, J. Power Sources 174 (2007) 560–564.
[32] J.S. Lee, N.D. Quan, J.M. Hwang, J.Y. Bae, H. Kim, B.W. Cho, H.S. Kim, H. Lee, Electrochem. Commun. 8 (2006) 460–464.
[33] H. Matsumoto, M. Yanagida, K. Tanimoto, M. Nomura, Y. Kitagawa, Y. Miyazaki, Chem. Lett. 29 (2000) 922–923.
[34] Z.-B. Zhou, H. Matsumoto, K. Tatsumi, Chem. - Eur. J. 10 (2004) 6581–6591.
[35] Z.-B. Zhou, H. Matsumoto, K. Tatsumi, Chem. - Eur. J. 11 (2005) 752–766.
[36] Z.-B. Zhou, H. Matsumoto, K. Tatsumi, Chem. - Eur. J. 12 (2006) 2196–2212.
[37] W.A. Henderson, J.V.G. Young, D.M. Fox, H.C. De Long, P.C. Trulove, Chem. Commun. (2006) 3708–3710.
[38] Z. Fei, W.H. Ang, D. Zhao, R. Scopelliti, E.E. Zvereva, S.A. Katsyuba, P.J. Dyson, J. Phys. Chem. B 111 (2007) 10095–10108.
[39] W. Xu, L.-M. Wang, R.A. Nieman, C.A. Angell, J. Phys. Chem. B 107 (2003) 11749–11756.
[40] H. Matsumoto, H. Sakaebe, K. Tatsumi, J. Power Sources 146 (2005) 45–50.
[41] K. Tsunashima, M. Sugiya, Electrochem. Commun. 9 (2007) 2353–2358.
[42] S. Fang, L. Yang, J. Wang, M. Li, K. Tachibana, K. Kamijima, Electrochim. Acta 54 (2009) 4269–4273.
[43] H.B. Han, K. Liu, S.W. Feng, S.S. Zhou, W.F. Feng, J. Nie, H. Li, X.J. Huang, H. Matsumoto, M. Armand, Z.B. Zhou, Electrochim. Acta 55 (2010) 7134–7144.
[44] K. Tsunashima, F. Yonekawa, M. Sugiya, Electrochem. Solid-State Lett. 12 (2009) A54–A57.
[45] K. Tsunashima, F. Yonekawa, M. Sugiya, Chem. Lett. 37 (2008) 314–315.
[46] S. Seki, Y. Ohno, H. Miyashiro, Y. Kobayashi, A. Usami, Y. Mita, N. Terada, K. Hayamizu, S. Tsuzuki, M. Watanabe, J. Electrochem. Soc. 155 (2008) A421–A427.
[47] S. Seki, Y. Kobayashi, H. Miyashiro, Y. Ohno, A. Usami, Y. Mita, M. Watanabe, N. Terada, Chem. Commun. (2006) 544–545.
[48] S. Seki, Y. Kobayashi, H. Miyashiro, Y. Ohno, Y. Mita, A. Usami, N. Terada, M. Watanabe, Electrochem. Solid-State Lett. 8 (2005) A577–A578.
[49] S. Ferrari, E. Quartarone, P. Mustarelli, A. Magistris, M. Fagnoni, S. Protti, C. Gerbaldi, A. Spinella, J. Power Sources 195 (2010) 559–566.
[50] T. Sato, T. Maruo, S. Marukane, K. Takagi, J. Power Sources 138 (2004) 253–261.
[51] T. Sato, G. Masuda, K. Takagi, Electrochim. Acta 49 (2004) 3603–3611.
[52] E. Stathatos, P. Lianos, V. Jovanovski, B. Orel, J. Photochem. Photobiol. A: Chem. 169 (2005) 57–61.
[53] J. Pernak, K. Sobaszkiewicz, J. Foksowicz-Flaczyk, Chem. - Eur. J. 10 (2004) 3479–3485.
[54] M. Kärnä, M. Lahtinen, J. Valkonen, J. Mol. Struct. 922 (2009) 64–76.
[55] H.-B. Han, K. Liu, S.-W. Feng, S.-S. Zhou, W.-F. Feng, J. Nie, H. Li, X.-J. Huang, H. Matsumoto, M. Armand, Z.-B. Zhou, Electrochim. Acta 55 (2010) 7134–7144.
[56] S. Fang, Y. Jin, L. Yang, S.-i. Hirano, K. Tachibana, S. Katayama, Electrochim. Acta 56 (2011) 4663–4671.
[57] S. Fang, Z. Zhang, Y. Jin, L. Yang, S.-i. Hirano, K. Tachibana, S. Katayama, J. Power Sources 196 (2011) 5637–5644.
[58] S. Fang, L. Yang, C. Wei, C. Jiang, K. Tachibana, K. Kamijima, Electrochim. Acta 54 (2009) 1752–1756.
[59] U. Schuchardt, R.M. Vargas, G. Gelbard, J. Mol. Catal. A: Chem. 99 (1995) 65–70.
[60] P. Wang, S.M. Zakeeruddin, M. Grätzel, W. Kantlehner, J. Mezger, E.V. Stoyanov, O. Scherr, Appl. Phys. A: Mater. Sci. Process. 79 (2004) 73–77.
[61] H. Xie, S. Zhang, H. Duan, Tetrahedron Lett. 45 (2004) 2013–2015.
[62] Y. Gao, S.W. Arritt, B. Twamley, J.n.M. Shreeve, Inorg. Chem. 44 (2005) 1704–1712.
[63] P. Bonhote, A.-P. Dias, N. Papageorgiou, K. Kalyanasundaram, M. Gratzel, Inorg. Chem. 35 (1996) 1168–1178.
[64] J.D. Holbrey, K.R. Seddon, J. Chem. Soc. Dalton Trans. (1999) 2133–2140.
[65] A.S. Larsen, J.D. Holbrey, F.S. Tham, C.A. Reed, J. Am. Chem. Soc. 122 (2000) 7264–7272.
[66] E.E. Paillard, Q. Zhou, W. Henderson, G.B. Appetecchi, M. Montanino, S. Passerini, ECS Trans. 16 (2009) 51–57.
[67] X.-G. Sun, S. Dai, Electrochim. Acta 55 (2010) 4618–4626.
[68] M.J. Monteiro, F.F.C. Bazito, L.J.A. Siqueira, M.C.C. Ribeiro, R.M. Torresi, J. Phys. Chem. B 112 (2008) 2102–2109.
[69] M.J. Monteiro, F.F. Camilo, M.C.C. Ribeiro, R.M. Torresi, J. Phys. Chem. B 114 (2010) 12488–12494.
[70] S. Fang, L. Yang, C. Wei, C. Peng, K. Tachibana, K. Kamijima, Electrochem. Commun. 9 (2007) 2696–2702.
[71] M. Moshkovich, Y. Gofer, D. Aurbach, J. Electrochem. Soc. 148 (2001) E155–E167.
[72] A. Fernicola, F. Croce, B. Scrosati, T. Watanabe, H. Ohno, J. Power Sources 174 (2007) 342–348.